Numerical comparison of the beam model and 2D linearized elasticity

Eva Fabijanić[†]

Pliva d.d.,10000 Zagreb, Croatia

Josip Tambača[‡]

Department of Mathematics, University of Zagreb, Bijenicka 30,10000 Zagreb, Croatia

Abstract.   In this paper we compare the solution of the one-dimensional beam model and the numerical solution of the two-dimensional linearized elasticity problem for rectangular domain of the beam-like form. We first derive the beam model starting from the two-dimensional linearized elasticity, the same way it is derived from the three-dimensional linearized elasticity. Then we present the numerical solution of the two-dimensional problem by finite element method. As expected the difference of two approximations becomes smaller as the thickness of the beam tends to zero. We then analyze the applicability of the one-dimensional model and verify the main properties of the beam modeling for thin beams.

Keywords: linearized elasticity; asymptotic expansion; beam model; numerical solution; finite elements.

1. Introduction

In order to apply the beam model (or any other lower-dimensional model) one needs to know how well it approximates the real problem. Let us assume the strains are small, so we are within the scope of linearized elasticity. Then we are left with the question of estimating the difference between the solution of the beam model and the corresponding problem of three-dimensional linearized elasticity for beam-like structure. This beam-like means that the structure is thin in two directions (thickness) comparing to the third (length). It is well known that the beam model is valid (approximation is good) if the beam is thin enough, i.e., if the ratio thickness/length is small enough. Still, there remains open a question of being "thin enough" (or "small enough"). This paper gives an answer to this question and puts some bounds on errors, comparing the solution of the beam model and the numerical solution of two-dimensional linearized elasticity (since the numerical solution, accurate enough, of the three-dimensional linearized elasticity is still out of reach).

Lower-dimensional modeling is well established approach for thin structures (beams, plates and

---

† E-mail: eva.fabijanic@pliva.hr
‡ Associate Professor, Ph.D., Corresponding author, E-mail: tambaca@math.hr

shells). Their geometry is "basically" lower-dimensional and allows for a small parameter (thickness) to be recognized. Very complex three-dimensional (or two-dimensional) model is then replaced by a simpler one, lower-dimensional model.

Despite of the rapid increase of the computational ability the beam model is widely used and serves as the keystone in many applications, like modeling of rotating shafts (e.g., see Hili *et al.* 2007, Gu and Cheng 2004, Vanegas Useche *et al.* 2007), modeling of frame structures (e.g., see Albarracín and Grossi 2005, Igawaa *et al.* 2004), modeling of nanotubes (e.g., see Rafii-Tabar 2004, Yoon *et al.* 2003), modeling of pipelines (e.g., see Iimura 2004, Andreuzzi and Perrone 2001). Moreover, the research based on the one-dimensional models of beam-like structures, including the Euler-Bernoulli beam, is still very attractive area (we mention some of recent publications Chen and Liu 2006, Kim 2004, Li and Guo 2008, Rajasekaran and Varghese 2005, Lu *et al.* 2008).

The usage of the lower-dimensional model instead of the three-dimensional one, of course, needs to be justified. Usually it is done by the convergence theorem, where one proves a certain convergence of the family of solutions of the three-dimensional problem, when the thickness tends to zero, to the solution of the lower-dimensional model. For linearized elasticity and beams see Aganović and Tutek 1986, Trabucho and Viaño 1996, for plates see Ciarlet and Destuynder 1979, Ciarlet 1990, for curved rods see Jurak and Tambača 1999 and Jurak and Tambača 2001 while for shells see Ciarlet 1997. Even where available, the error estimates between the solution of the three-dimensional problem and the solution of the model, do not answer to the applicability of the model. Namely, the constant in the error estimate is usually unknown so we can not tell when the structure is thin enough so it can be modeled by the lower-dimensional model.

The purpose of this paper is to give an answer to the question when the beam is thin enough so the one-dimensional model can be used. We do it by comparing the numerical approximation of the linearized elasticity problem for beam-like structures and the associated one-dimensional problem. In doing so we need to solve numerically the linearized elasticity problem with an error of the numerical approximation which is of smaller order then the error of the one-dimensional model with respect to the linearized elasticity problem. Unfortunately, the three-dimensional linearized elasticity is still out of reach for such precision. Therefore we focus on the two-dimensional linearized elasticity problem on a rectangle and the one-dimensional model derived by taking one side of the rectangle to zero. The obtained model (4) for transversal displacement is of the same structure as the one widely known which is derived from the three-dimensional elasticity, with different elastic constant (see Section 2). We also derive the form of the first and the second corrector and state the main convergence theorem (Theorem 2.1). As the model is derived from the two-dimensional linearized elasticity its use is very limited, but the conclusions of the rate of approximation should be useful. Note here that we are focused only on the model of transversal displacements of beams and not on the extension of beams (which is of smaller order).

For the two-dimensional linearized elasticity problem in rectangle we use the open source finite element package FreeFEM++ (see http://www.freefem.org) and solve it numerically by the finite element method using P2 Lagrangian elements and for constant density of the body force. Then we compare the numerical solution with the model. The approximation agrees with the convergence results from the Theorem 2.1. Moreover, we are able to test the classical properties that appear in the lower-dimensional modeling in linearized elasticity, namely, the unshearability of the cross-sections of the beam and the Kirchhoff-Love form of the displacement. For instance, the model approximates the behavior of the middle line in two-dimensional linearized elasticity problem with the relative error of 3% for beams with the width to length ratio less then $\frac{1}{20}$. The first

approximation (0th order model plus 1th order corrector - that is the form of the Kirchhoff-Love displacement) behaves the same way on the whole rectangle (not only on the middle line). Moreover, the angle between the deformed cross-sections and the deformed middle line for beams with the width to length ratio less then $\frac{1}{20}$ is never less then 89.5 degrees.

2. Derivation of 1D beam model

In this section we sketch the asymptotic derivation of the 1D beam model and present the main convergence results starting from the 2D linearized elasticity. The obtained model is not the same as in the case of derivation from the 3D linearized elasticity, so its use is very limited. The derivation is essentially the same as in the case of three-dimensional elasticity performed in the case of curved rods in Jurak and Tambača 1999 and Jurak and Tambača 2001, so we do not present it in detail but just sketch the main steps.

Let $\varepsilon > 0$ and

$$\Omega^{\varepsilon} = <0, 1> \times <-\frac{\varepsilon}{2}, \frac{\varepsilon}{2}>$$

be 2D beam-like domain. We assume $\overline{\Omega}^{\varepsilon}$ to be the linearized elastic body with the Lamé coffiecients λ and μ, subjected to the volume force with density f^{ε}. We assume the beam is clamped on both bases $B_0^{\varepsilon} = \{0\} \times <-\frac{\varepsilon}{2}, \frac{\varepsilon}{2}>$, $B_1^{\varepsilon} = \{1\} \times <-\frac{\varepsilon}{2}, \frac{\varepsilon}{2}>$. Then the displacement of the beam $\boldsymbol{u}^{\varepsilon}$ belongs to the function space

$$V_0(\Omega^{\varepsilon}) = \{\boldsymbol{v} \in H^1(\Omega^{\varepsilon})^2 : \boldsymbol{v}|_{x_1 = 0} = \boldsymbol{v}|_{x_1 = 1} = 0\}$$

and satisfies the variational equation

$$\int_{\Omega^{\varepsilon}} \mathcal{C}\mathbf{e}(\boldsymbol{u}^{\varepsilon}) \cdot \mathbf{e}(\boldsymbol{v})dx = \int_{\Omega^{\varepsilon}} \boldsymbol{f}^{\varepsilon} \cdot \boldsymbol{v}dx, \quad \boldsymbol{v} \in V_0(\Omega^{\varepsilon}) \tag{1}$$

here $\mathbf{e}(\boldsymbol{v}) = 1/2(\nabla\boldsymbol{v} + \nabla\boldsymbol{v}^T)$ is the symmetrized gradient and $\mathcal{C}$ is the elasticity tensor

$$\mathcal{C}\mathbf{E} = \lambda\text{tr}(\mathbf{E})\mathbf{I} + 2\mu\mathbf{E}, \quad \mathbf{E} \in \text{Sym}(2)$$

This is a classical problem of linearized elasticity. For the volume force $\boldsymbol{f}^{\varepsilon} \in L^2(\Omega^{\varepsilon})$ it possess a unique solution.

In order to derive the 1D model we follow the standard technique as in Ciarlet and Destuynder 1979 and apply the asymptotic expansion method to this problem rewritten on the canonical domain

$$\Omega = <0, 1> \times <-\frac{1}{2}, \frac{1}{2}>$$

independent of ε. Let $\mathbf{R}^{\varepsilon}(y_1, y_2) = (y_1, \varepsilon y_2)$. The function

$$\boldsymbol{u}(\varepsilon) = \boldsymbol{u}^{\varepsilon} \circ \mathbf{R}^{\varepsilon} \in V_0(\Omega) = \{\boldsymbol{v} \in H^1(\Omega)^2 : \boldsymbol{v}|_{y_1 = 0} = \boldsymbol{v}|_{y_1 = 1} = 0\}$$

is the unique solution of the problem

$$\int_{\Omega} \mathcal{C}\mathbf{e}^{\varepsilon}(\boldsymbol{u}(\varepsilon)) \cdot \mathbf{e}^{\varepsilon}(\boldsymbol{v})dy = \int_{\Omega} \boldsymbol{f}(\varepsilon) \cdot \boldsymbol{v}dy, \quad \boldsymbol{v} \in V_0(\Omega) \tag{2}$$

here $f(\varepsilon) = f^{\varepsilon} \circ R^{\varepsilon}$ and

$$\mathbf{e}^{\varepsilon}(v) = \frac{1}{\varepsilon}\gamma_{-1}(v) + \gamma_0(v)$$

$$\gamma_{-1}(v) = \begin{pmatrix} 0 & \dfrac{1}{2}\dfrac{\partial v_1}{\partial y_2} \\ \dfrac{1}{2}\dfrac{\partial v_1}{\partial y_2} & \dfrac{\partial v_2}{\partial y_2} \end{pmatrix}, \quad \gamma_0(v) = \begin{pmatrix} \dfrac{\partial v_1}{\partial y_1} & \dfrac{1}{2}\dfrac{\partial v_2}{\partial y_1} \\ \dfrac{1}{2}\dfrac{\partial v_2}{\partial y_1} & 0 \end{pmatrix}$$

To obtain the family of solutions $(u(\varepsilon))_{\varepsilon > 0}$ which is bounded in $L^2(\Omega)^2$, (see Jurak and Tambača 1999), a special asymptotic of the body force is needed

$$f(\varepsilon) = \varepsilon^2 f \qquad (3)$$

where f is independent of ε. This is the strongest force density allowed with all components equally scaled.

We assume that

$$u(\varepsilon) = u^0 + \varepsilon u^1 + \ldots$$

and proceed then in several steps inserting special test functions into Eq. (2) and considering the equation obtained as the coffiecient of the lowest power of ε. In the first step we insert $u(\varepsilon)$ as the test function and consider the equation which is the coffiecient of ε^{-2}:

$$\int_{\Omega} \mathcal{C}\gamma_{-1}(u^0) \cdot \gamma_{-1}(u^0) dx = 0$$

As $\mathcal{C}$ is positive definite it implies $\gamma_{-1}(u^0) = 0$, so we conclude that $u^0(y_1, y_2) = w^0(y_1)$ for $w^0 \in H_0^1(0,1)^2$.

In the second step we repeat the same procedure and consider the equation which is the coffiecient of ε^0:

$$\int_{\Omega} \mathcal{C}(\gamma_{-1}(u^1) + \gamma_0(u^0)) \cdot (\gamma_{-1}(u^1) + \gamma_0(u^0)) dx = 0$$

It follows $\gamma_{-1}(u^1) + \gamma_0(u^0) = 0$ which implies

$$u^0(y_1, y_2) = \begin{pmatrix} 0 \\ w_2^0(y_1) \end{pmatrix}, \quad u^1(y_1, y_2) = \begin{pmatrix} -(w_2^0)'(y_1)y_2 + w_1^1(y_1) \\ w_2^1(y_1) \end{pmatrix}$$

where w^1 is an arbitrary function of y_1, $w^1 \in H_0^1(0,1)^2$. The form of the approximation $u^0 + \varepsilon u^1$ for the functions above is the so-called Kirchhoff-Love displacement.

In the third step we just take from Eq. (2) the equation which is the coffiecient of ε^0:

$$\int_{\Omega} \mathcal{C}(\gamma_{-1}(u^2) + \gamma_0(u^1)) \cdot \gamma_{-1}(v) dy = 0, \quad v \in V_0(\Omega)$$

It is then easy to conclude that

$$(\mathcal{C}(\gamma_{-1}(u^2) + \gamma_0(u^1)))_{12} = (\mathcal{C}(\gamma_{-1}(u^2) + \gamma_0(u^1)))_{22} = 0$$

It follows

$$\frac{\partial u_1^2}{\partial y_2} + \frac{\partial u_2^1}{\partial y_1} = 0, \quad \lambda\Big(\frac{\partial u_1^1}{\partial y_1} + \frac{\partial u_2^2}{\partial y_2}\Big) + 2\mu\frac{\partial u_2^2}{\partial y_2} = 0$$

i.e.,

$$\boldsymbol{u}^2(y_1, y_2) = \begin{pmatrix} -(w_2^1)'(y_1)y_2 + w_1^2(y_1) \\ -\dfrac{\lambda}{\lambda+2\mu}\Big(-(w_2^0)''(y_1)\dfrac{y_2^2}{2} + (w_1^1)'(y_1)y_2\Big) + w_2^2(y_1) \end{pmatrix}$$

where $\boldsymbol{w}^2$ is an arbitrary function of y_1, $\boldsymbol{w}^2 = H^1(0,1)^2$. Note here that we do not prescribe any boundary condition for $\boldsymbol{w}^2$ as we did for $\boldsymbol{w}^0$ and $\boldsymbol{w}^1$. It should be determined by the boundary layer, which we do not discuss here.

Finally we insert the test function of the form

$$\boldsymbol{v} = \boldsymbol{v}^0 + \varepsilon\boldsymbol{v}^1, \quad \boldsymbol{v}^0(y_1, y_2) = \begin{pmatrix} 0 \\ v_2^0(y_1) \end{pmatrix}, \quad \boldsymbol{v}^1(y_1, y_2) = \begin{pmatrix} -(v_2^0)'(y_1)y_2 \\ 0 \end{pmatrix}$$

in Eq. (2), where $v_2^0 \in H_0^2(0,1)$. The lowest order power in the equation is then 2 and its coffiecient gives the equation

$$\int_\Omega \mathcal{C}(\gamma_{-1}(\boldsymbol{u}^2) + \gamma_0(\boldsymbol{u}^1)) \cdot \gamma_0(\boldsymbol{v}^1)dy = \int_\Omega \boldsymbol{f} \cdot \boldsymbol{v}^0 dy, \quad v_2^0 \in H_0^2(0,1)$$

Using calculated form of $\boldsymbol{u}^0$, $\boldsymbol{u}^1$, $\boldsymbol{u}^2$ it is equivalent to

$$\int_\Omega 4\mu\frac{\lambda+\mu}{\lambda+2\mu}(-(w_2^0)''y_2 + (w_1^1)')(-(v_2^0)'')y_2 dy = \int_\Omega f_2 v_2^0 dy, \quad v_2^0 \in H_0^2(0,1)$$

The definition of Ω implies that the term with w_1^1 disappears from the equation an that the model for transversal displacement is given by: find $w_2^0 \in H_0^2(0,1)$ such that

$$4\mu\frac{\lambda+\mu}{\lambda+2\mu}\frac{1}{12}\int_0^1 (w_2^0)''(v_2^0)''dy_1 = \int_0^1 \overline{f_2}v_2^0 dy, \quad v_2^0 \in H_0^2(0,1) \tag{4}$$

where $\overline{f_2} = \int_{-1/2}^{1/2} f_2 dy_2$. Note here that the only difference in the model with respect to the one derived from three-dimensional elasticity is in the coffiecient in the equation of the model (EI in 3D case).

Using the same technique as in the modeling of curved rods from three-dimensional linearized elasticity Jurak and Tambača 2001 the convergence theorems can be obtained. We collect all results in the following theorem.

Theorem 2.1 Let $\boldsymbol{u}(\varepsilon) \in V_0(\Omega)$ for $0 < \varepsilon$ be the solution of the variational Eq. (2). Then

$$\boldsymbol{u}(\varepsilon) \to \boldsymbol{u}^0 \quad \text{in} \quad V_0(\Omega) \quad \text{strongly,}$$

$$\frac{1}{\varepsilon}\gamma^\varepsilon(\boldsymbol{u}(\varepsilon)) \to \gamma^0 \quad \text{in} \quad L^2(\Omega)^9 \quad \text{strongly,}$$

where $\boldsymbol{u}^0 = (0, w_2^0)$, $w_2^0 \in H_0^2(0,1)$ is the solution of Eq. (4) and γ^0 is given by

$$\gamma^0 = \gamma_{-1}(\boldsymbol{u}^2) + \gamma_0(\boldsymbol{u}^1) = \begin{pmatrix} 1 & 0 \\ 0 & -\dfrac{\lambda}{\lambda+2\mu} \end{pmatrix}(-(w_2^0)''y_2)$$

Remark 2.1 Note that the form of γ^0 implies that $w_1^1 = 0$. Moreover, note that f_1 does not play any role here. It actually appears on the right hand side of the problem for w_2^1 in the form of the line density of the moment as well as on the right hand side of the problem for w_1^2.

Remark 2.2 According to the model the undeformed cross-section at $(x_1, 0)$ is the line connecting points $(x_1, -\varepsilon/2)$ and $(x_1, \varepsilon/2)$. Considering the zeroth order approximation and the first corrector after deformation it remains straight line connecting the points $(x_1 + (w_2^0)'(x_1)\varepsilon/2, -\varepsilon/2 + w_0(x_1))$ and $(x_1 - (w_2^0)'(x_1)\varepsilon/2, \varepsilon/2 + w_0(x_1))$. Therefore the vector connecting the edges is

$$(-(w_2^0)'(x_1)\varepsilon, \varepsilon)$$

The deformed middle line is parameterized by $(x_1, w_2^0(x_1))$, so the tangent line at this point is given by $(1, (w_2^0)'(x_1))$. Therefore in the first approximation the deformed cross-sections remain perpendicular to the deformed middle line.

If we denote

$$\hat{\boldsymbol{u}}(\varepsilon) = \boldsymbol{u}^0 + \varepsilon \boldsymbol{u}^1 + \varepsilon^2 \boldsymbol{u}^2$$

from the convergence of $\gamma^\varepsilon(\boldsymbol{u}(\varepsilon))$ follows that

$$\frac{1}{\varepsilon}\gamma^\varepsilon(\boldsymbol{u}(\varepsilon) - \hat{\boldsymbol{u}}(\varepsilon)) \to 0 \quad \text{in} \quad L^2(\Omega)^9 \text{ strongly,}$$

where

$$\boldsymbol{u}^1(y_1, y_2) = \begin{pmatrix} -(w_2^0)'(y_1)y_2 \\ 0 \end{pmatrix}, \quad \boldsymbol{u}^2(y_1, y_2) = \begin{pmatrix} 0 \\ \dfrac{\lambda}{\lambda + 2\mu}(w_2^0)''(y_1)\dfrac{y_2^2}{2} \end{pmatrix}$$

Note that $\boldsymbol{w}^1$, and $\boldsymbol{w}^2$ are not necessary for this convergence.

These results can be rephrased at the physical domain Ω^ε. Let $\hat{\boldsymbol{u}}^\varepsilon = \hat{\boldsymbol{u}}(\varepsilon) \circ (\mathbf{R}^\varepsilon)^{-1}$ and denote a seminorm by

$$\|\boldsymbol{v}\|_0 = \sqrt{\left\|\frac{\partial \boldsymbol{v}}{\partial x_1}\right\|_{L^2(\Omega^\varepsilon)^2}^2 + \varepsilon^2 \left\|\frac{\partial \boldsymbol{v}}{\partial x_2}\right\|_{L^2(\Omega^\varepsilon)^2}^2}$$

Then

$$\frac{1}{\varepsilon^{1/2}}\|\boldsymbol{u}^\varepsilon - \boldsymbol{u}^0\|_{L^2(\Omega^\varepsilon)^2} \to 0 \tag{5}$$

$$\frac{1}{\varepsilon^{1/2}}\|\boldsymbol{u}^\varepsilon - \boldsymbol{u}^0\|_0 \to 0 \tag{6}$$

$$\frac{1}{\varepsilon^{3/2}}\|\mathbf{e}(\boldsymbol{u}^\varepsilon - \hat{\boldsymbol{u}}^\varepsilon)\|_{L^2(\Omega^\varepsilon)^4} \to 0 \tag{7}$$

In the first convergence $\boldsymbol{u}^0$ could be replaced by $\hat{\boldsymbol{u}}^\varepsilon$ and the better order convergence is expected. To obtain such an analytical estimate some more complicated work should be done including construction of boundary layers.

3. Numerical method for 2D linearized elasticity

In this section we describe the numerical method used for 2D linearized elasticity problem Eq. (2), i.e., Eq. (1). We solve them by finite element method using the open source finite element package FreeFEM++. The code we use is the one from the Freefem++ manual, Hecht, Pironneau, Le Hyaric and Ohtsuka 2005, Example 10, page 40, but in difference we use $P2$ elements.

In the following section we consider behavior of the numerical solution of Eq. (1), i.e., Eq. (2), as ε tends to zero. Let $i \in \mathbb{N}$. In the sequel we consider only $\varepsilon = 1/i$.

As the relation between the Lamé coefficients and the load is linear we are allowed to rescale them. We take the Young modulus and the Poisson ratio to be

$$E = 1, \quad \nu = 0.3 \tag{8}$$

For the volume force we consider densities of the form

$$\boldsymbol{f}^{\varepsilon} = -2\varepsilon^{2} \tag{9}$$

as the asymptotic analysis performed in the previous section requires this behavior. In this case $\boldsymbol{f}(\varepsilon) = -2\varepsilon^{2}$. The factor 2 is chosen just to obtain displacements which can be easily observed.

Now we need to choose which variational problem we solve numerically, the one on thin domain Ω^{ε} given by Eq. (1), or the one on the canonical domain Ω given by Eq. (2). The domain in any case is rectangle with one side of unit length. The mesh is chosen in the regular way as in the Fig. 1 with vertical edge divided in j equal subintervals and the horizontal edge divided in $i * j$ equal subintervals (in Fig. 1 $j = 3$ and $i = 2$). The fact that we take i times more nodes on the horizontal edge is natural in order to have triangles with all angles not too small.

According to the Table 1 numerical solutions of Eq. (1) and Eq. (2) agree up to the relative difference of 10^{-6} for the parameters we are interested, so in the sequel we consider the solutions on the thin domain Ω^{ε} only, i.e., Eq. (1). We also denote $\|\boldsymbol{v}\|_{\infty} = \sup_{x \in \Omega^{\varepsilon}} \sqrt{v_1(x)^2 + v_2(x)^2}$.

The next task is to set the parameter j for which we will obtain numerical solution of Eq. (1) which is good enough for all ε, i.e., i considered.
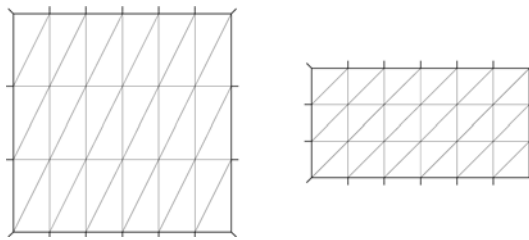

Fig. 1 The canonical Ω and thin Ω^{ε} domain for $\varepsilon = 1/2$

Table 1 Relative sup difference of the solutions on the canonical and thin domain with P2 elements

i	10	20	40	80	160
$\Delta_{\infty}, j = 5$	4.18e-012	6.07e-011	7.56e-010	1.12e-008	6.36e-008
$\Delta_{\infty}, j = 10$	2.49e-011	3.06e-010	3.81e-009	2.19e-008	2.40e-007
$\Delta_{\infty}, j = 20$	7.17e-011	5.16e-010	4.12e-009	7.70e-008	1.20e-006

Table 2 Relative errors of solutions of Eq. (1) by $P2$ elements on two meshes

i	10	20	40	80	160
Δ_∞, $j = 5$	0.00232	0.00108	0.00052	0.00025	0.00012
Δ_∞, $j = 10$	0.00140	0.00036	0.00017	8.4e-005	4.2e-005
Δ_∞, $j = 20$	0.00078	0.00019	4.9e-005	2.3e-005	1.7e-005
Δ_2, $j = 5$	0.00265	0.00125	0.00060	0.00029	0.00014
Δ_2, $j = 10$	0.00089	0.00042	0.00020	9.6e-005	4.8e-005
Δ_2, $j = 20$	0.00024	0.00011	5.6e-005	2.6e-005	1.8e-005
Δ_0, $j = 5$	0.00604	0.00226	0.00086	0.00035	0.00015
Δ_0, $j = 10$	0.00353	0.00128	0.00046	0.00017	6.8e-005
Δ_0, $j = 20$	0.00196	0.00071	0.00024	8.8e-005	3.4e-005
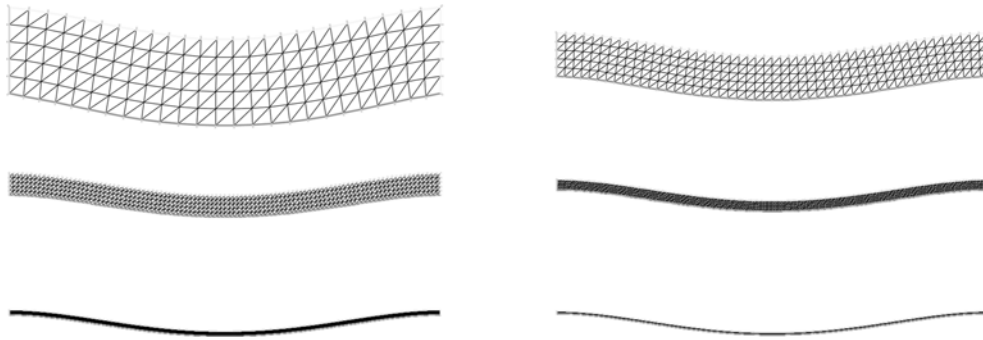
Fig. 2 Solutions of Eq. (1) for $i = 5$, 10, 20, 40, 80, 160 and $j = 5$

We compare the solution of Eq. (1) by $P2$ elements for $j = 5$, 10, 20 with the solution by $P2$ elements for $j = 40$ for different values of i. The relative sup, $L^2(\Omega^\varepsilon)$ and $V_0(\Omega^\varepsilon)$ differences are presented in Table 2. It follows that for $j = 20$ all problems we will consider, namely $i = 10$, 20, 40, 80, 160 are numerically solved with the relative error of order 10^{-3}.

At the end of this section note, in Fig. 2, the form of the solution for different thickness, namely for $i = 5$, 10, 20, 40, 80, 160 and $j = 5$ (force density is chosen according to Eq. (9)).

4. Numerical comparison

In this section we compare numerical solution of Eq. (1) with the approximation built through the asymptotic analysis in Section 2. Especially we are interested in justification of conclusions derived there about convergences (5)-(7) and the property of Kirchhoff-Love displacement, namely that the cross-sections remain approximately rigid and perpendicular to the deformed middle curve. Finally we check how thin the beam should be so the difference between the solution of 3D problem and the model is less then 3%. This is possible as in Section 3 we estimated the error of the numerical solution to be of order 10^{-3}.

All numerical computations are done for the data from Section 3, namely Eq. (8) and Eq. (9) and for $j = 20$. For given force density solution of the model (4) is given by

$$w_2^0(y_1) = -\frac{\lambda + 2\mu}{4\mu(\lambda + \mu)}(1 - y_1)^2 y_1^2$$

Therefore

$$\boldsymbol{u}^{\varepsilon, 0}(x_1, x_2) = \boldsymbol{u}^0 \circ (\boldsymbol{R}^{\varepsilon})^{-1}(x_1, x_2) = \begin{pmatrix} 0 \\ -\dfrac{\lambda + 2\mu}{4\mu(\lambda + \mu)}(1 - x_1)^2 x_1^2 \end{pmatrix}$$

$$\boldsymbol{u}^{\varepsilon, 1}(x_1, x_2) = \varepsilon \boldsymbol{u}^1 \circ (\boldsymbol{R}^{\varepsilon})^{-1}(x_1, x_2) = \begin{pmatrix} \dfrac{\lambda + 2\mu}{4\mu(\lambda + \mu)}(2 - 6x_1 + 4x_1^2)x_1 \\ 0 \end{pmatrix} x_2$$

$$\boldsymbol{u}^{\varepsilon, 2}(x_1, x_2) = \varepsilon^2 \boldsymbol{u}^2 \circ (\boldsymbol{R}^{\varepsilon})^{-1}(x_1, x_2) = \begin{pmatrix} 0 \\ -\dfrac{\lambda}{4\mu(\lambda + \mu)}(2 - 12x_1 + 12x_1^2) \end{pmatrix}\frac{x_2^2}{2}$$

First we want to check the convergence from Theorem 2.1, i.e., corresponding convergences (5)-(7) rewritten on the thin domain. In Table 3 we compare the numerical solution of Eq. (1) and approximation by $\boldsymbol{u}^0$. The results suggest the convergence is linear, i.e., $\|\boldsymbol{u}^{\varepsilon} - \boldsymbol{u}^{\varepsilon, 0}\| \leq C\varepsilon$ for all norms, with the constant in the equation of order 1. In the Fig. 3 the pointwise error in the Euclid norm is plotted.

Zeroth order approximation consists only of the transversal displacement. Therefore all cross-sections are just translated. The first corrector accounts for the rotation of the cross-sections. If we add it the convergence improves to quadratic, i.e., $\|\boldsymbol{u}^{\varepsilon} - \boldsymbol{u}^{\varepsilon, 0} - \boldsymbol{u}^{\varepsilon, 1}\| \leq C\varepsilon^2$, with constant of order 10,

Table 3 Relative difference of solutions of Eq. (1) and the model (4)

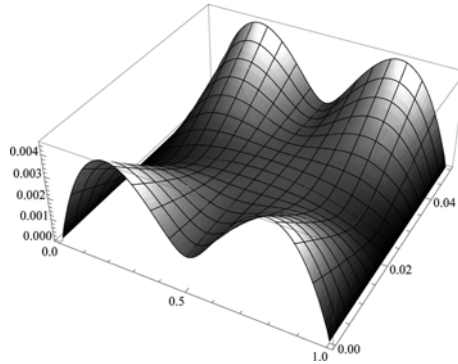| i	10	20	40	80	160
$\|\boldsymbol{u}^{\varepsilon} - \boldsymbol{u}^{\varepsilon, 0}\|_{\infty}$	0.15721	0.07713	0.03843	0.01922	0.00961
$\|\boldsymbol{u}^{\varepsilon} - \boldsymbol{u}^{\varepsilon, 0}\|_{2}$	0.15158	0.05789	0.02574	0.01252	0.00624
$\|\boldsymbol{u}^{\varepsilon} - \boldsymbol{u}^{\varepsilon, 0}\|_{0}$	0.22009	0.10697	0.05304	0.02649	0.01325

Fig. 3 Pointwise error in the Euclid norm of the 0th order approximation ($i = 20$)

Table 4 Relative difference of solutions of Eq. (1) and the model (4) with the first corrector

i	10	20	40	80	160
$\left\| u^{\varepsilon} - u^{\varepsilon,0} - u^{\varepsilon,1} \right\|_{\infty}$	0.11257	0.02877	0.00627	0.00102	5.75e-005
$\left\| u^{\varepsilon} - u^{\varepsilon,0} - u^{\varepsilon,1} \right\|_{2}$	0.12440	0.03212	0.00700	0.00113	4.06e-005
$\left\| u^{\varepsilon} - u^{\varepsilon,0} - u^{\varepsilon,1} \right\|_{0}$	0.11741	0.03082	0.00722	0.00157	0.00042
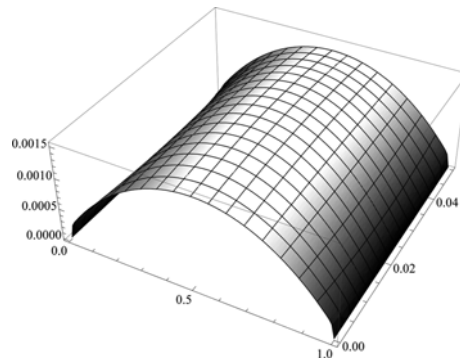
Fig. 4 Pointwise error in the Euclid norm of the 1st order approximation (i = 20)

see Table 4. This convergence rate is a consequence of w^1 being zero (actually w_2^1 being zero, as w_1^1 always is). Note here that the error of the numerical solution for i = 160 and the error of the model are of the same order, i.e., the error can not be improved unless j is increased (and more accurate numerical solution is obtained). Pointwise error of this first order approximation is plotted in Fig. 4.

Second order corrector is obtained by the requirement that symmetrized gradient is approximated, see Eq. (7). It accounts for the stretching of the cross-sections. This approximation does not improve the convergence of the approximation of the displacement for sup, L^2 and V_0 norms as can be seen from the Table 5. Moreover, it introduces the error at the fixed ends of the beam due to the boundary layer, see Fig. 5. For i = 20 the error introduced is still smaller then the overall error, but for i = 160 the boundary layer error dominates. The data from Table 6 suggests that the convergence (7) is linear in ε.

As it is suggested by the shape of the error at Fig. 3 the sup error on the middle line of the beam is smaller then the overall sup error. Therefore we compare u^{ε} and u^0 only on the middle line and do it with and without of averaging u^{ε} over the cross-section. The results are presented in Table 7. There is no difference in averaging the solution on the cross-section or not. Moreover, u^0

Table 5 Relative difference of solutions of Eq. (1) and the model (4) with two correctors

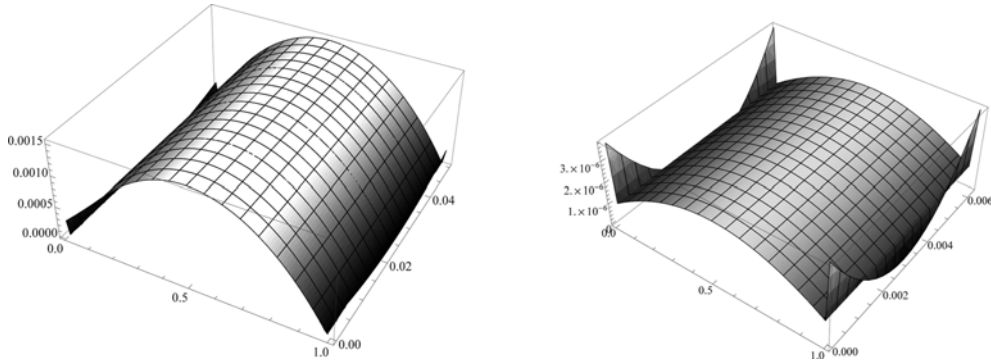| i	10	20	40	80	160
$\left\| u^{\varepsilon} - \hat{u}^{\varepsilon} \right\|_{\infty}$	0.11270	0.02878	0.00627	0.00102	6.69e-005
$\left\| u^{\varepsilon} - \hat{u}^{\varepsilon} \right\|_{2}$	0.12584	0.03251	0.00710	0.00115	3.31e-005
$\left\| u^{\varepsilon} - \hat{u}^{\varepsilon} \right\|_{0}$	0.12521	0.03291	0.00772	0.00167	0.00042

Fig. 5 Pointwise error in the Euclid norm of the 2nd order approximation ($i = 20$ and $i = 160$)

Table 6 Relative difference of symmetrized gradient of the numerical solution and the model with two correctors

i	10	20	40	80	160
$\left\| \dfrac{1}{\varepsilon} \mathbf{e}(\boldsymbol{u}^{\varepsilon} - \hat{\boldsymbol{u}}^{\varepsilon}) \right\|_2$	0.45054	0.24696	0.13235	0.07304	0.04279

Table 7 Relative difference of solutions of Eq. (1) and the model (4)

i	10	20	40	80	160
$\left\| \boldsymbol{u}^{\varepsilon} - \boldsymbol{u}^{\varepsilon,0} \right\|_{\infty}$	0.15721	0.07713	0.03843	0.01922	0.00961
$\left\| \boldsymbol{u}^{\varepsilon} - \boldsymbol{u}^{\varepsilon,0} - \boldsymbol{u}^{\varepsilon,1} \right\|_{\infty}$	0.11257	0.02877	0.00627	0.00102	5.7e-005
$\left\| \boldsymbol{u}^{\varepsilon} \right|_{x_2=0} - \boldsymbol{u}^0 \right\|_{L^{\infty}(0,1)}$	0.12685	0.02962	0.00631	0.00102	2.4e-005
$\left\| \dfrac{1}{\varepsilon} \int_{-\frac{\varepsilon}{2}}^{\frac{\varepsilon}{2}} \boldsymbol{u}^{\varepsilon} dx_2 - \boldsymbol{u}^0 \right\|_{L^{\infty}(0,1)}$	0.12405	0.02891	0.00613	0.00098	3.5e-005

Table 8 Relative difference of solutions of Eq. (1) and the model (4) on the middle line

i	15	16	17	18	19	20	21	22	23	24	25
$100 \left\| \boldsymbol{u}^{\varepsilon} - \boldsymbol{u}^{\varepsilon,0} - \boldsymbol{u}^{\varepsilon,1} \right\|_{\infty}$	5.1	4.5	4.0	3.5	3.2	2.8	2.5	2.3	2.1	1.9	1.7
$100 \left\| \boldsymbol{u}^{\varepsilon} \right|_{x_2=0} - \boldsymbol{u}^{\varepsilon,0} \right\|_{L^{\infty}(0,1)}$	5.4	4.7	4.1	3.7	3.3	2.9	2.6	2.4	2.1	1.9	1.8

approximates the middle line at the same order as the approximation with the first corrector.

In Table 8 are relative differences between the model and the numerical solution of Eq. (1). For instance, for $i = 20$ the relative difference is below 3%, so for $\varepsilon \leq 1/20$ we may say the beam is thin.

In Table 9 the maximal cosine of the angle between the deformed middle line and the deformed cross-section for the numerical solution of Eq. (1) is given (end-points of the cross-section are used in calculation of the angle). As expected the maximal value is for the thickest beam ($i = 10$), and corresponds to 1.5 degrees, as the unshearability of the cross-section holds only for beams which are thin enough. Note that for $i = 5$ maximal angle is with cosine equal to 0.09109 (about 5

Table 9 Maximal cosine of the angle between the deformed middle line and the deformed cross-section for the
numerical solution of Eq. (1)

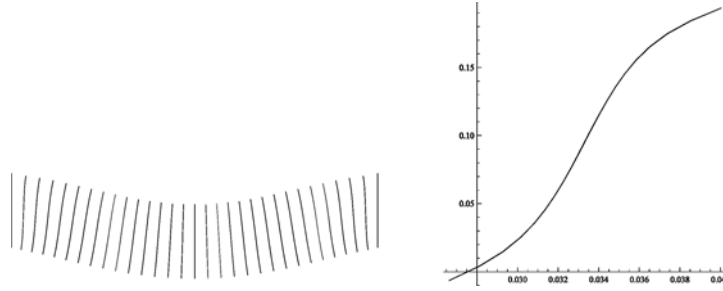| i	10	20	40	80	160
$\sup_{x1}\cos(\angle)$	0.02494	0.00664	0.00317	0.00206	0.00115

Fig. 6 Deformed cross-sections of the beam

degrees). The deformed cross-sections are in Fig. 6, plotted for beam with $i = 5$ just to stress its
form. Real shape of the cross-section can be seen on the right figure, but note the different scales.

5. Conclusions

The main purpose of this paper is to analyze the applicability of the beam model for thin beam-
like linearized elastic bodies and to put some bounds on the errors between the solution of the beam
model and numerical solution of the two-dimensional linearized elasticity problem for thin
rectangles.

First we derive the one-dimensional model starting from the two-dimensional linearized elasticity
problem on a thin rectangular domain. We formulate the zeroth order model and its corrector. The
solution of the two-dimensional linearized elasticity problem on a thin domain is denoted by u^{ε}, the
solution of zeroth order model by $u^{\varepsilon,0}$ and the correctors by $u^{\varepsilon,1}$. The comparison of the finite
element method solution of the two-dimensional problem with the exact solution of the one-
dimensional model suggests

1) the one dimensional model approximates the two-dimensional problem with the order ε, i.e.,
$\left\| u^{\varepsilon} - u^{\varepsilon,0} \right\|_{\infty} \leq C\varepsilon$,

2) the one dimensional model with correctors approximates the two-dimensional problem with the
order ε^2, i.e., $\left\| u^{\varepsilon} - u^{\varepsilon,0} - u^{\varepsilon,1} \right\|_{\infty} \leq C\varepsilon^2$,

3) the second corrector does not improve the error estimate,

4) the solution of the one dimensional model approximates the behavior of the solution of the
two-dimensional problem on the middle line with the order ε^2,

5) for the beam with $\frac{width}{length}$ ratio less then of $\frac{1}{20}$ the solution of the beam model with correctors
approximates the solution of two-dimensional problem with an error which is less then 3%,

6) for the beam with $\frac{width}{length}$ ratio less then of $\frac{1}{20}$ the solution of the zeroth order model (the beam
model) approximates the solution of two-dimensional problem at the middle line with an error
which is less then 3%,

7) the correctors correct the rotation of the cross-sections of the beam. For beams with $\frac{width}{length}$ ratio less then $\frac{1}{10}$ the deformed cross-section remains orthogonal on the deformed middle line with an error which is less then 1.5 degrees.

References

Aganović, I. and Tutek, Z. (1986), "A justification of the one-dimensional linear model of elastic beam", *Math. Method. Appl. Sci.*, **8**, 1-14.

Albarracín, C.M. and Grossi, R.O. (2005), "Vibrations of elastically restrained frames", *J. Sound Vib.*, **285**, 467-476.

Andreuzzi, F. and Perrone, A. (2001), "Analytical solution for upheaval bucklingin burried pipeline", *Comput. Meth. Appl. Mech. Eng.*, **190**, 5081-5087.

Chen, D.W. and Liu, T.L. (2006), "Free and forcedvibrations ofa tapered cantilever beam carrying multiple point masses", *Struct. Eng. Mech.*, **23**(2), 209-216.

Ciarlet, P.G. (1990), *Mathematical Elasticity, Vol. II: Theory of Plates*, North-Holland.

Ciarlet, P.G. (1997), *Mathematical Elasticity, Vol. III: Theory of Shells*, North-Holland.

Ciarlet, P.G. and Destuynder, P. (1979), "A justification of the two dimensional linear plate model", *J. Mécanique*, **18**, 315-344.

Gu, U.C. and Cheng, C.C. (2004), "Vibration analysis of a high-speed spindle under the action of a moving mass", *J. Sound Vib.*, **278**, 1131-1146.

Hecht, F., Pironneau, O., Le Hyaric, A. and Ohtsuka, K. (2005), *Freefem++ manual*, http://www.freefem.org/ff++.

Hili, M.A., Fakhfakh, T. and Haddar, M. (2007), "Vibration analysis of a rotating exible shaft-disk system", *J. Eng. Math.*, **57**, 351-363.

Igawaa, H., Komatsub, K., Yamaguchia, I. and Kasaia, T. (2004), "Wave propagation analysis of frame structures using the spectral element method", *J. Sound Vib.*, **277**, 1071-1081.

Iimura, S. (2004), "Simplified mechanical model for evaluating stress in pipeline subject to settlement", *Constr. Build. Mater.*, **18**, 469-479.

Jurak, M. and Tambača, J. (1999), "Derivation and justification of a curved rod model", *Math. Model. Meth. Appl. Sci.*, **9**(7), 991-1014.

Jurak, M. and Tambača, J. (2001), "Linear curved rod model. General curve", *Math. Model. Meth. App. Sci.*, **11**(7), 1237-1252.

Kim, J.T. (2004), "Identification of prestress-loss in PSC beams using modal information", *Struct. Eng. Mech.*, **17**(3-4), 467-482.

Li, G.Q. and Guo, S.X. (2008), "Analysis of restrained steel beams subjected to heating and cooling. Part I: Theory", *Steel Compos. Struct.*, **8**(1), 1-18.

Lu, Z.R., Liu, J.K. and Law, S.S. (2008), "Identification of prestress force in a prestressed Timoshenko beam", *Struct. Eng. Mech.*, **29**(3), 241-258.

Rafii-Tabar, H. (2004), "Computational modelling of thermo-mechanical and transport properties of carbon nanotubes", *Phys. Rep.*, **390**, 235-452.

Rajasekaran, S. and Varghese, S.P. (2005), "Damage detection in beams and plates using wavelet transforms", *Comput. Concrete*, **2**(6), 481-498.

Trabucho, L. and Viaño, J.M. (1996), *Mathematical Modelling of Rods*, in Handbook of Numerical Analysis, Vol. IV, Eds. P.G. Ciarlet, J. L. Lions, North-Holland.

Vanegas Useche, L.V., Abdel Wahab, M.M. and Parker, G.A. (2007), "Dynamics of an unconstrained oscillatory flicking brush for road sweeping", *J. Sound Vib.*, **307**, 778-801.

Yoon, J., Ru, C.Q. and Mioduchowski, A. (2003), "Vibration of an embedded multiwall carbon nanotube", *Compos. Sci. Technol.*, **63**, 1533-1542.